

## TOWARDS IMPROVED CONTRAIL PARAMETERIZATIONS FOR CLIMATE-SCALE MODELS

David P. Duda

National Institute of Aerospace, Hampton, Virginia

Patrick Minnis

NASA Langley Research Center, Hampton, Virginia

Lance A. Avey

Science Systems and Applications, Inc., Hampton, Virginia

### 1. INTRODUCTION

Contrails remain one of the most uncertain impacts of aviation on climate. Most previous attempts to simulate contrail climate effects on the global scale have estimated contrail cirrus coverage as a function of the model's relative humidity. Although the atmospheric conditions necessary for contrail formation are well defined, the diagnosis or prediction of such clouds is still complicated by uncertainties in modeling the atmospheric state in the upper troposphere. Considerable uncertainty remains in coverage estimates by climate-model-scale simulations.

This study assesses the use of relative humidity with respect to ice (RHI) derived from hourly, high-resolution numerical weather prediction (NWP) analyses, including the RUC (Rapid Update Cycle) model (Benjamin et al., 2004) and the ARPS (Advanced Regional Prediction System) model (Xue et al., 2003) to estimate contrail occurrence. Contrail occurrence measured from high-resolution satellite imagery is related to upper tropospheric relative humidity computed in the NWP analyses by a simple linear regression. This regression is then used to reconstruct the contrail occurrence frequency based on the upper tropospheric relative humidity fields computed in the NWP analyses.

### 2. METHODOLOGY

We use the automated contrail detection algorithm of Mannstein et al. (1999) to detect linear contrails within 1-km resolution satellite data. Two sets of satellite data are studied.

Forty-nine afternoon overpasses of NOAA-16 AVHRR (Advanced Very High Resolution Radiometer) imagery from November 2005 are analyzed with the Mannstein et al., algorithm, as well as twenty-three multi-spectral images from *Aqua* and *Terra* MODIS (MODerate resolution Imaging Spectroradiometer) measurements taken from daytime and nighttime overpasses between September and December 2007. The contrail detection results from the AVHRR data are sorted into 0.5×0.5 degree grid boxes extending from 130 to 65 W, and from 25 to 55 N. The horizontal domain of the MODIS data extends from 90 to 75 W, and from 30 to 42 N.

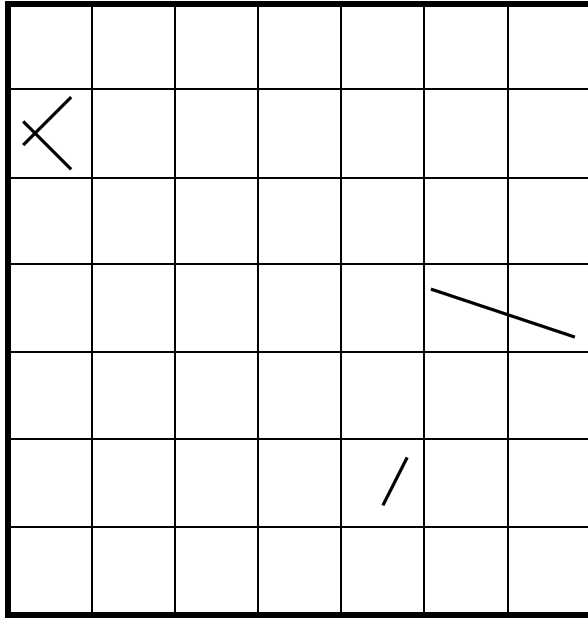
The grid boxes are then grouped into sets of 7×7 arrays of boxes, and a contrail occurrence fraction ( $C_{occur}$ ) within each array is computed. To maximize the number of arrays, maximum overlap is used such that a single MODIS image could have as many as  $(30-6) \times (24-6) = 432$  arrays. The AVHRR data contains a total of 102,767 arrays while the MODIS data has 8,208 arrays. The contrail occurrence fraction is defined as the ratio between the number of grid boxes within the array that contain at least one identified contrail and the total number of grid boxes in the array. Figure 1 shows an example of the contrail occurrence fraction computed for a grid box array.

Relative humidity data from the RUC and ARPS analyses are then compared to the  $C_{occur}$  results. Humidity data is selected from the analysis closest to the overpass time so that the temporal difference between satellite and NWP data is always 30 minutes or less. The mean RHI in the layer from 200 to 300 hPa is computed for each grid box from the model analyses ( $RHI_{box}$ ), and then averaged over each 7×7 array ( $RHI_{array}$ ). The layer from 200 to 300 hPa was selected because most commercial air

---

\* Corresponding author address: David P. Duda, NASA Langley Research Center, Mail Stop 420, Hampton, VA 23681; e-mail: dduda@nianet.org

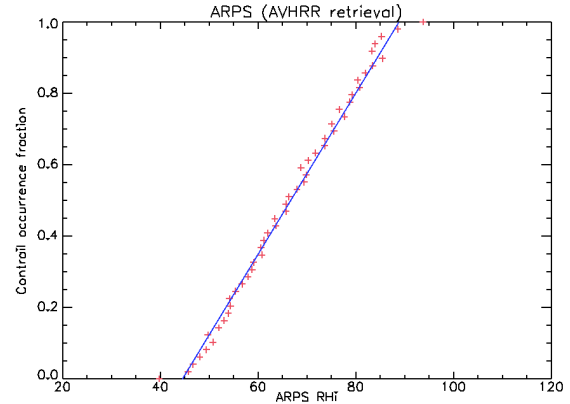
traffic over the United States flies between these levels (Garber et al., 2005). The grid box arrays are then sorted by contrail occurrence fraction (50 possible values), and the  $RHI_{array}$  for each fraction are then averaged to obtain a mean  $RHI_{array}$  for each contrail occurrence fraction category ( $\overline{RHI_{array}}$ ).



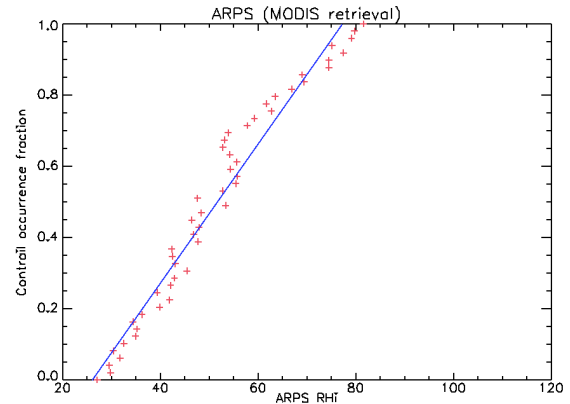
**Figure 1.** Schematic of 7×7 grid box array with identified linear contrails. The contrail occurrence fraction in this example is  $4/49 = 0.08$ .

Plots of the contrail occurrence fraction versus the  $\overline{RHI_{array}}$  computed from each model show a strong correlation between model humidity and the probability of contrail occurrence within a region. Figures 2 and 3 show the relationship between  $\overline{RHI_{array}}$  and  $C_{occur}$  for the ARPS model. The results for the RUC model (not shown) are similar. The correlation is better for the AVHRR data because the number of grid box arrays is more than 10 times larger than for the MODIS data. This close relationship suggests that the layer-mean upper tropospheric humidity may be used as a proxy for contrail occurrence fraction. Thus, it may be possible to reconstruct the climatological  $C_{occur}$  over a region from RUC or ARPS relative humidity climatologies.

We test this hypothesis by comparing the contrail occurrence fraction derived directly from the AVHRR and MODIS imagery with the occurrence fraction fields derived from the

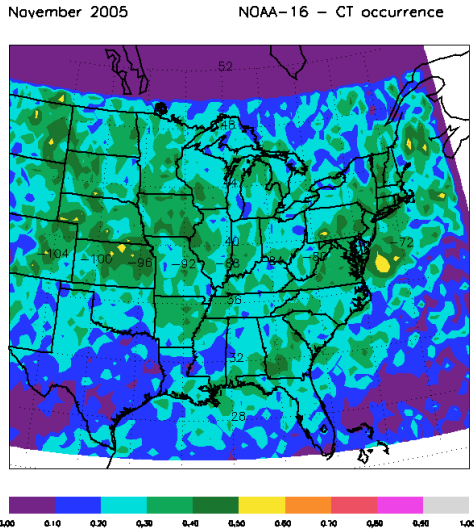


**Figure 2.** Plot of contrail occurrence fraction versus the mean of the  $RHI_{array}$  values computed for each occurrence fraction category from the ARPS analyses. RHI values are derived from the NWP data for each 7×7 grid box array within the AVHRR imagery.

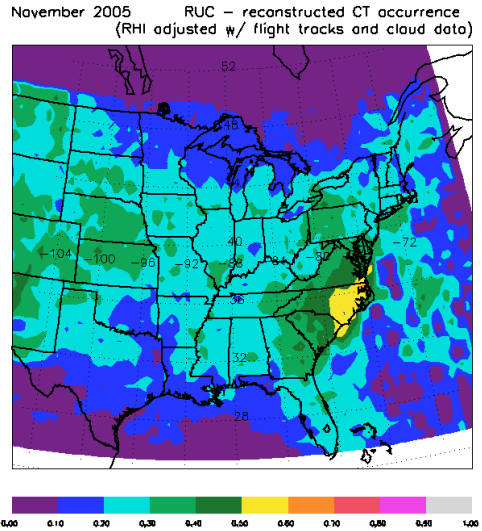


**Figure 3.** Same as Figure 2, but for MODIS retrievals.

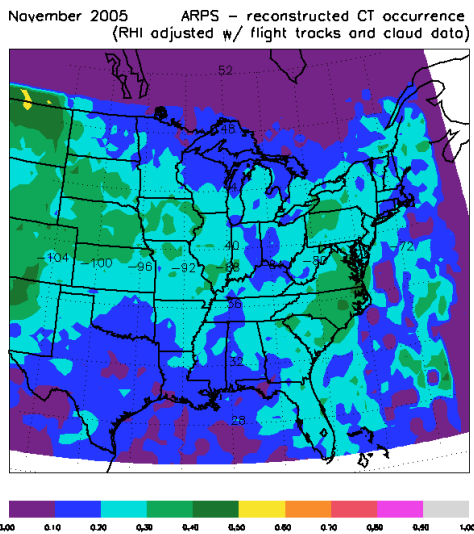
ARPS and RUC RHI data. The mean 200 to 300 hPa humidity (from both NWP models) is computed for each 0.5×0.5 degree grid box that contains valid satellite contrail detection data. In addition to the relative humidity data, the reconstructions use estimates of commercial flight track data (Garber et al., 2005) to mask out regions of no air traffic, and cloud coverage data from the GOES 0.5 degree VISST gridded cloud product dataset (Minnis et al., 2005) to remove areas of thick cloud cover that would block the automated contrail detection method. Grid boxes without any flight tracks longer than 40 km within the last two hours before each satellite overpass were excluded from the contrail occurrence reconstructions. Grid boxes with greater than 70 percent cloud coverage and a mean optical thickness greater than 3 were also excluded from the reconstructions.



**Figure 4.** Contrail occurrence frequency observed from 49 afternoon overpasses of NOAA-16 AVHRR imagery using the Mannstein et al. automated contrail detection algorithm during November 2005.



**Figure 6.** Same as Figure 5, but based on RUC RHI data.



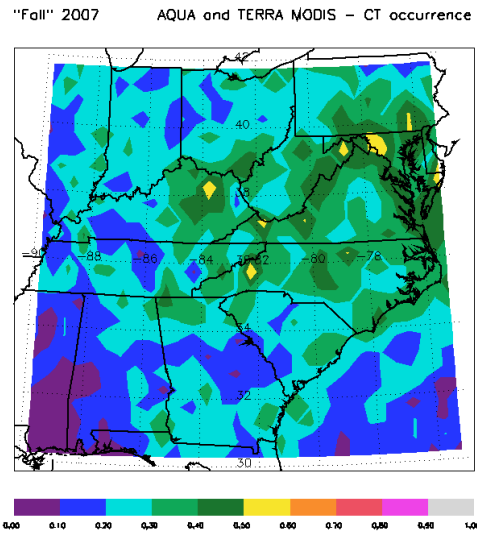
**Figure 5.** Reconstructed contrail occurrence frequency for the November 2005 AVHRR overpass times based on ARPS RHI data adjusted with flight track and cloud coverage data.

Figure 4 presents the observed contrail occurrence fractions for the November 2005 AVHRR overpasses, while Figures 5 and 6 show the reconstructed  $C_{occur}$  derived from the ARPS and RUC RHI data, respectively. The reconstructed fields have slightly lower contrail occurrence values than the observed field, although the general distribution of contrail occurrence is similar. Both the observed and reconstructed fields have broad maxima over

the northern Great Plains, minima along the Mississippi River valley and over Texas, and another area of broad maxima along the East Coast states. The eastern maxima in Figure 4, however, are situated further north than the East Coast maxima in the reconstructed fields. Another difference between the observed and reconstructed fields is the observed maximum in  $C_{occur}$  off the coast of the Middle Atlantic States that is not in Figures 5 or 6. This region is east of a major air traffic corridor, and it is likely that this area results from the advection of the maximum in  $C_{occur}$  visible in the reconstructed fields over eastern Virginia and eastern North Carolina.

The contrail occurrence fractions observed during the MODIS overpasses from the September through December 2007 are shown in Figure 7, and the corresponding ARPS and RUC reconstructed fields are presented in Figures 8 and 9. The observed contrail fractions are significantly larger than the reconstructed values, especially over the northeastern quadrant of the analysis region. The automated contrail detection algorithm appears to be more sensitive to cloud streets in the MODIS imagery, and may contain more false positive errors than in the AVHRR imagery. During the late fall and winter, this region often produces low-to-mid level cloud streets as cold air outbreaks flow over the mountains in western Pennsylvania and West Virginia. The contrail occurrence fractions reconstructed from the RUC data are slightly

larger than those from the ARPS data, but the overall structure of both fields are similar.



**Figure 7.** Same as Figure 4, but the contrail occurrence frequency was observed from 23 day and night overpasses of *Aqua* and *Terra* MODIS imagery between September and December 2007.

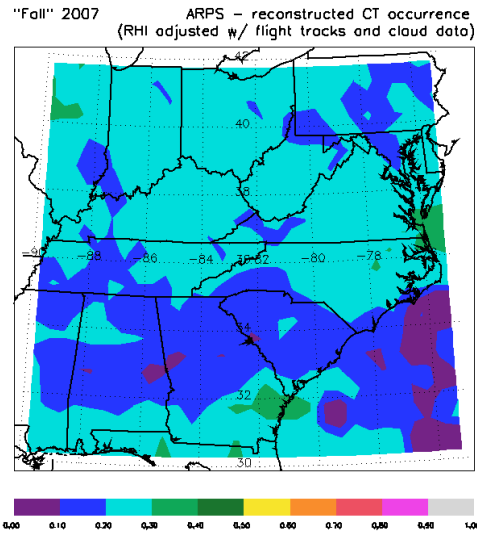


**Figure 8.** Same as Figure 5, but the reconstructed contrail occurrence frequency is based on ARPS data taken from the MODIS overpass times.

### 3. DISCUSSION

The results presented here suggest that the mean RHI fields from NWP analyses can be used to reconstruct the general contrail occurrence frequency across the United States once the effects of air traffic and thick cloud cover are accounted for. An interesting result of

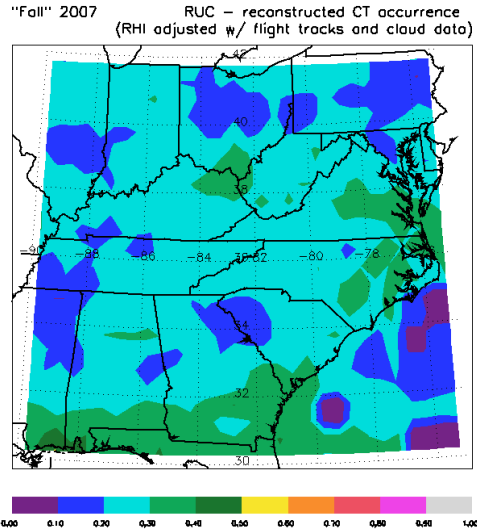


**Figure 9.** Same as Figure 8, but the reconstructed contrail occurrence frequency is based on RUC data.

this study is that it demonstrates the large differences in upper tropospheric humidity that can appear in NWP analysis as operational models evolve. A comparison of Figures 2 and 3 show that the ARPS model humidity analyses are considerable drier in 2007 (MODIS overpasses) than in 2005.

More work is needed to refine the technique, and to improve the contrail detection algorithm. Avey et al. (2008) discusses some methods to improve the Mannstein et al. method and reduce the number of misidentifications. Other atmospheric variables are important for contrail persistence including vertical velocity, temperature, and atmospheric lapse rate. The inclusion of these and other variables may improve the reconstructions. Other sources of upper tropospheric relative humidity information such as the Atmospheric Infrared Sounder (AIRS) (Chahine et al., 2006) may provide improved reconstructions, and we plan to compare reconstructions using AIRS humidities to the RUC/ARPS results in the near future.

### Acknowledgements

This material is based upon work supported by NAS contracts NAG-02044 and NCC-1-02043 NIA-2579.

The authors wish to thank Donald Garber for the flight track data, and Kirk Ayers and Mandana Khaiyer for their help in producing the gridded GOES VISST cloud data products.

## References

- Avey, L. A., R. Palikonda, P. Minnis, and D. P. Duda, 2008: Linear contrail detection over the eastern United States from AVHRR and MODIS data. Proc. AMS 13th Conf. Aviation Range and Aerospace Meteorology, New Orleans, LA, Jan. 20-24, P1.4.
- Benjamin, S. G., D. Dévényi, S. S. Weygandt, K. J. Brundage, J. M. Brown, G. A. Grell, D. Kim, B. E. Schwartz, T. G. Smirnova, T. L. Smith, and G. S. Manikin, 2004b: An hourly assimilation-forecast cycle: The RUC. Mon. Wea. Rev., **132**, 495-518.
- Chahine, M. T. and others, 2006: AIRS – Improving weather forecasting and providing new data on greenhouse gases. Bull. Amer. Meteorol. Soc., **87**, 911-926.
- Donald P. Garber, Patrick Minnis, and P. Kay Costulis, 2005: A commercial flight track database for upper tropospheric aircraft emission studies over the USA and southern Canada. Meteorologische Zeitschrift, Vol. 14, No. 4 (August 2005), 445-452.
- Mannstein, H., R. Meyer, P. Wendling, 1999: Operational detection of contrails from NOAA-AVHRR data. Int. J. Remote Sensing, **20**, 1641-1660.
- Minnis, P., et al., 2001: A near-real time method for deriving cloud and radiation properties from satellites for weather and climate studies. Proc. AMS 11th Conf. Satellite Meteorology and Oceanography, Madison, WI, Oct. 15-18, 477-480.  
[http://www-pm.larc.nasa.gov/arm\\_refs.html#CPR](http://www-pm.larc.nasa.gov/arm_refs.html#CPR)
- Xue, M., D.-H. Wang, J.-D. Gao, K. Brewster, and K. K. Droegemeier, 2003: The Advanced Regional Prediction System (ARPS), storm-scale numerical weather prediction and data assimilation, Meteor. Atmos. Physics, **82**, 139-170.